Journal of South American Earth Sciences 63 (2015) 385–399

Contents lists available at ScienceDirect

Journal of South American Earth Sciences

journal homepage: www.elsevier.com/locate/jsames

Evolution of Irruputuncu volcano, Central Andes, northern Chile

I. Rodríguez [a, b, *], O. Roche [b], S. Moune [b], F. Aguilera [c], E. Campos [a], M. Pizarro [d]

[a] Departamento de Ciencias Geológicas, Facultad de Ingeniería y Ciencias Geológicas, Universidad Católica del Norte, Av. Angamos #0610, Antofagasta, Chile
[b] Laboratoire Magmas et Volcans, Université Blaise Pascal-CNRS-IRD, OPGC, 5 rue Kessler 63038, Clermont-Ferrand, France
[c] Servicio Nacional de Geología y Minería, Santa María 0104, Santiago, Chile
[d] Programa de Doctorado en Ciencias mención Geología, Universidad de Chile, Plaza Ercilla 803, Santiago, Chile

ARTICLE INFO

Article history:
Received 31 March 2015
Received in revised form
16 July 2015
Accepted 28 August 2015
Available online 5 September 2015

Keywords:
Irruputuncu volcano
Central Andes
Debris avalanche
Block and ash flow
Lava flow

ABSTRACT

The Irruputuncu is an active volcano located in northern Chile within the Central Andean Volcanic Zone (CAVZ) and that has produced andesitic to trachy-andesitic magmas over the last ~258 ± 49 ka. We report petrographical and geochemical data, new geochronological ages and for the first time a detailed geological map representing the eruptive products generated by the Irruputuncu volcano. The detailed study on the volcanic products allows us to establish a temporal evolution of the edifice. We propose that the Irruputuncu volcanic history can be divided in two stages, both dominated by effusive activity: Irruputuncu I and II. The oldest identified products that mark the beginning of Irruputuncu I are small-volume pyroclastic flow deposits generated during an explosive phase that may have been triggered by magma injection as suggested by mingling features in the clasts. This event was followed by generation of large lava flows and the edifice grew until destabilization of its SW flank through the generation of a debris avalanche, which ended Irruputuncu I. New effusive activity generated lavas flows to the NW at the beginning of Irruputuncu II. In the meantime, lava domes that grew in the summit were destabilized, as shown by two well-preserved block-and-ash flow deposits. The first phase of dome collapse, in particular, generated highly mobile pyroclastic flows that propagated up to ~8 km from their source on gentle slopes as low as 11° in distal areas. The actual activity is characterized by deposition of sulfur and permanent gas emissions, producing a gas plume that reaches 200 m above the crater. The maximum volume of this volcanic system is of ~4 km^3, being one of the smallest active volcano of Central Andes.

1. Introduction

The Central Andean Volcanic Zone (CAVZ) corresponds to a magmatic arc generated by partial melting of the asthenosphere due to subduction of the Nazca plate beneath the South American plate (Coira et al., 1982). The convergence between these two plates has been accompanied by orogeny and crustal thickening during the last ~27.5 Ma (Allmendinger et al., 1997; Wörner et al., 2000). Irruputuncu (20°45′ S; 68°34′ W; 5165 m a.s.l) is a small active composite stratovolcano located in the CAVZ, at the Chile–Bolivia border (Fig. 1). According to de Silva and Francis (1991), the volcanic edifice is composed mainly by andesitic and dacitic lava flows, dacitic lava domes, block-and-ash and pyroclastic flow deposits. Available published ages of Irruputuncu formations range from 0.14 ± 0.04 Ma for a lava dome on the upper western flank (K–Ar method, Wörner et al., 2000) to 1570 ± 900 years BP for a fresh block-and-ash flow deposit on the southwestern flank (^{14}C method, Stern et al., 2007). The Irruputuncu complex is built on the Ujina and Pastillos ignimbrites formed during upper Miocene and Pleistocene, respectively (Vergara and Thomas, 1984). Vergara and Thomas (1984) considered that Irruputuncu volcano was part of *Estrato-volcanes III* unit that includes two other volcanoes (Pabellón del Inca and Poruñita), that have perfectly preserved cones and solfataric activity, and whose dacitic to andesitic rocks contain hornblende and pyroxene.

Irruputuncu has two craters aligned NE–SW (de Silva and Francis, 1991), the southernmost is still being active and has a diameter of 200 m (González-Ferrán, 1995). The present activity is

* Corresponding author. Departamento de Ciencias Geológicas, Facultad de Ingeniería y Ciencias Geológicas, Universidad Católica del Norte, Av. Angamos #0610, Antofagasta, Chile.
E-mail address: irodriguez@ucn.cl (I. Rodríguez).

http://dx.doi.org/10.1016/j.jsames.2015.08.012
0895-9811/

characterized by deposition of sulfur and permanent gas emissions, with SO_2 as the main phase (Clavero et al., 2006). Fumaroles reach 200 m above the crater (Aguilera, 2008). Their outlet temperature varies between 83 °C and 240 °C while gas phases consist of highly concentrated SO_2 and H_2S (170 and 52 μmol/mol, respectively) and less abundant HCl, N_2, HF, O_2 and CH_4 (Tassi et al., 2011). Chemical and isotopic compositions of the gases indicate mixing between magmatic, hydrothermal and atmospheric fluids, as typically observed in volcanic systems in convergent margins (Tassi et al., 2011).

Although the Irruputuncu has historical eruptive activity reported in the literature (de Silva and Francis, 1991), there are no clear references of large scale historical eruptions. However, persistent heat flux in a hot spring NW from the summit in the Pastillos Ignimbrite unit, as well as ash fall deposits on the NW flank of the volcano show evidences of recent magmatic activity (de Silva and Francis, 1991). In December 1989 a press report published in Bolivia mentioned a possible eruption of the volcano, but this information was never confirmed, while on March 25, 1990, fumarolic activity in the Irruputuncu crater was reported (BGVP, 1990). The first accurate description of volcanic activity corresponds to small phreatomagmatic explosions (increase in the volcanic activity) on November 26, 1995, which produced a 1000-m high ash-vapor plume (Global Volcanism Bulletin of Global Volcanism Program, 1997). After several minutes, the plume color turned to white and the material ejected was dispersed very slowly eastwards (BGVP, 1997). Recently, local inhabitants reported that a thermal spring located 13 km west of the volcano described by Hauser (1997) disappeared after an earthquake of magnitude 7.9 occurred in this area on June 13, 2005.

Few geochemical and petrological investigations, as well as, few radiometric ages have been reported for the Irruputuncu (Wörner et al. 1992, 2000; Mamani et al. 2008, 2010), which limits the understanding of the temporal evolution of the edifice. In order to overcome this issue, field campaigns were done in 2011 and 2012 to identify the main geological units and collect samples for radiometric dating as well as for petrological and geochemical analyses. In this paper, we present a detailed description of Irruputuncu geology (summarized in a map, with scale 1:50.000), 27 data of bulk rock geochemistry (14 new geochemistry data and 13 data compiled from Wörner et al., 1992; Mamani et al., 2008, 2010), and 7 radiometric ages data, corresponding to 4 new $^{40}Ar-^{39}Ar$ ages, 2 K–Ar and one ^{14}C age compiled from Wörner et al. (2000) and Stern et al. (2007). The goals of our contribution are: (i) provide complementary geochemical data of the main Irruputuncu eruptive units, (ii) report new Ar–Ar ages in order to reconstruct the eruptive history of this volcano, and (iii) provide a first detailed geological map of Irruputuncu. Our aim is to report the main characteristics of the Irruputuncu units, which may serve as a guide for further detailed investigations. Therefore, a detailed discussion on processes of magma generation, storage condition, and eruptive dynamics is beyond the scope of this paper.

2. Irruputuncu geological setting

Irruputuncu volcano is built over the Ujina and Pastillos ignimbrites (Vergara and Thomas, 1984). The Ujina Ignimbrite is a ~150 m thick pink to gray welded pyroclastic deposit containing mainly pumice fragments, and crystals (plagioclase, sanidine, quartz, hornblende and biotite). This deposit has been dated by K–Ar method (in biotite) at 9.3 ± 0.4 Ma (upper Miocene; Vergara and Thomas, 1984). The Pastillos Ignimbrite is 20–90 m thick and is formed by a lower member that is a light gray to white pumice-rich pyroclastic deposit, and an upper member dominated by cinerites that contain claystones, siltstones and finely stratified diatomites. The lower member has an age of 0.79 ± 0.2 Ma to 0.73 ± 0.16 Ma (K–Ar in biotite; Baker and Francis, 1978; Vergara and Thomas, 1984), while the upper member was dated at 0.32 ± 0.25 Ma (K–Ar in biotite; Wörner et al. 2000), corresponding to Middle Pleistocene.

At least two other older volcanic sequences have been recognized in the Irruputuncu volcano area (Baker and Francis, 1978; Vergara and Thomas, 1984). The first is the *Volcanic Group I*, corresponding to strongly eroded andesitic–dacitic volcanic edifices of middle to upper Miocene age. The second is the *Volcanic Group II*, constituted by moderately eroded volcanic edifices formed mainly by pyroxene-hornblende andesites and dacites. Examples of these units are the Pliocene Laguna and Bofedal volcanoes, located immediately northeast and southeast of Irruputuncu volcano. We found outcrops of the *Volcanic Group I* in the southwestern and southern flanks of Irruputuncu volcano, which are partially covered by Irruputuncu products (Fig. 2). These outcrops are strongly hydrothermally altered and correspond to: i) porphyritic dacitic lava flows containing plagioclase (18% vol.), biotite (10% vol.), hornblende (~5% vol.) and quartz (2% vol.) phenocrysts, and a groundmass (65% vol.) formed by glass, microlites of plagioclase and opaque minerals, and ii) hydrothermal breccia constituted by andesitic rock fragments (30% vol.) in a fine size matrix (70% vol.). Both dacitic lavas and hydrothermal breccias are moderately-to-strongly altered, with mineral assemblage mainly constituted by limonite, hematite and clays. Additionally, solfataric alteration is characterized by abundant native sulfur, which suggests that these outcrops could represent the core of an older, deeply eroded volcanic edifice.

3. Analytical methods

3.1. Geochemical analysis

A total of forty thin sections from representative samples of the Irruputuncu volcano were prepared at the Departamento de Geología, Universidad de Atacama, Chile, for petrographic description. The mineral proportions in percentage were determined using a polarized light microscope. Fourteen samples, each representative of a particular stage of the evolution of the Irruputuncu volcano, were selected for whole rock composition analysis by inductively couple plasma-atomic emission spectrometry (ICP-AES) at the Laboratoire Magmas et Volcans (LMV), Clermont Ferrand, France. Accuracy of measurements was verified by analyzing an international geological reference material provided by the USGS (Hawaii basalt, BHVO-1) and the 2σ uncertainty was in the range of 5–10%. Results are presented in Table 1.

The compositions of anorthite plagioclase crystals from some units of the Irruputuncu volcano were determinated at LMV on a SX-100 CAMECA electron microprobe (EMPA) using 15 kV accelerating voltage. A mixture of standard minerals (synthetic and natural) and glasses (A-THO and VG2) was used for calibration (see Óladottir et al., 2011, for further details).

3.2. Geochronology

Four unaltered representative samples were selected for $^{40}Ar/^{39}Ar$ geochronology (Table 2). Analyses were done at Argon Geochronology Lab, Oregon State University (OSU), USA. Groundmass glasses were selected from the sieved fraction <500 μm and all distinct phenocrysts were eliminated by handpicking to obtain a pure glass sample. Biotites were separated from the sieve fraction between 100 μm and 500 μm by handpicking. Samples (biotite or groundmass) were processed following the method described in Jordan and Grunder (2004). Note that sanidines, which are more

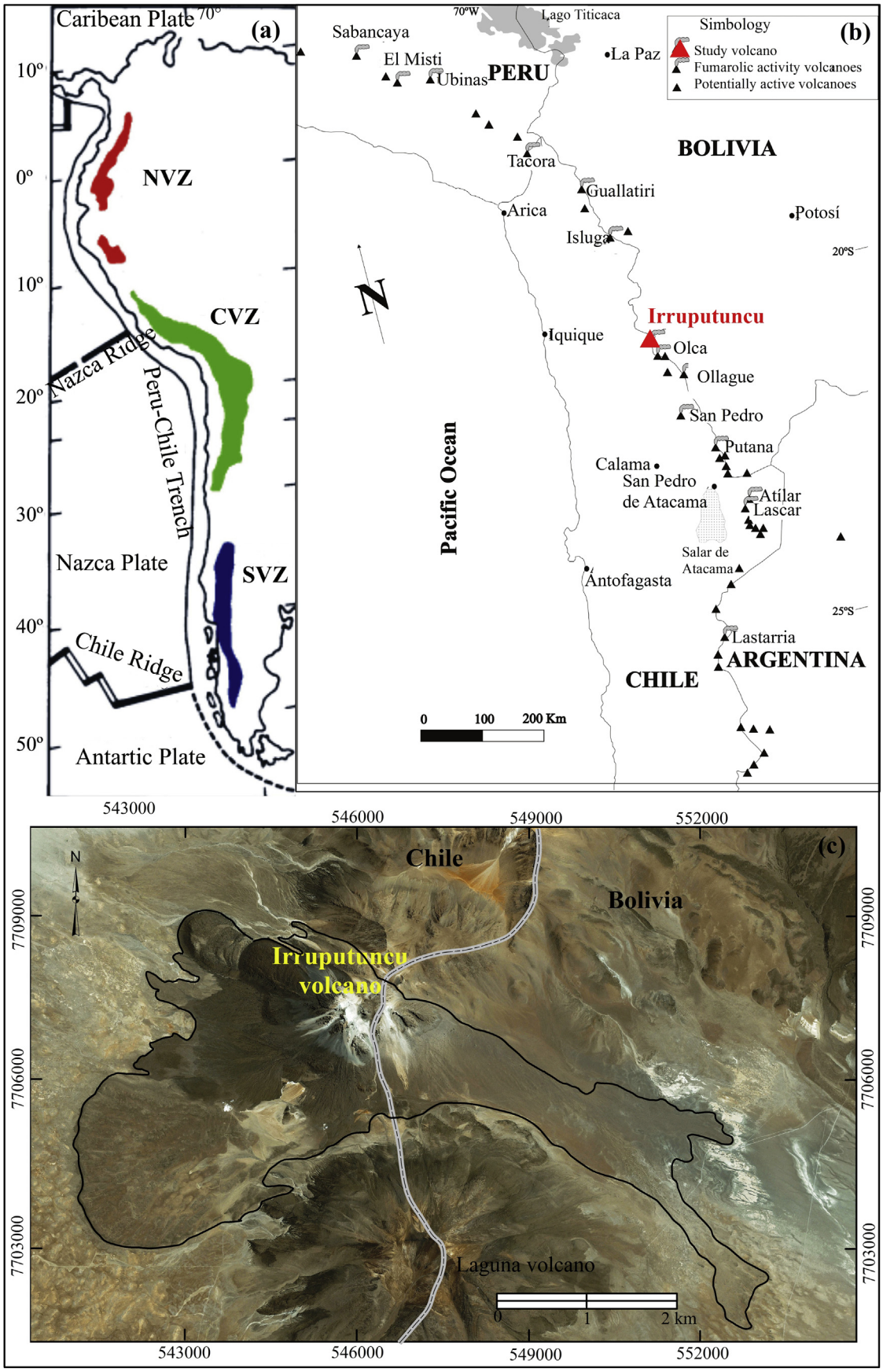

Fig. 1. (a) Map of the Andes, distribution of Northern (NVZ), Central (CVZ) and Southern Volcanic Zone (SVZ). Modified from de Silva and Francis, 1991. (b) Location of Irruputuncu volcano. Modified from Tassi et al., 2009. (c) Google Satellite image of Irruputuncu Volcanic Complex. Black lines show the limits of Irruputuncu volcano deposits.

suitable than biotites for Ar analyses, were lacking in our samples.

Three on four of the plateau ages are concordant (within the errors) with isochron ages (Table 2). In accordance with standard procedures at the Oregon State University laboratory we accept these plateau ages as the preferred ages. One sample (IRRU-46-A, Table 2), however, yielded a plateau age that failed to overlap (within the errors) with its isochron age; therefore, the isochron age with a lower MSWD (Mean Square of Weighted Deviates) is preferred. Note also that the age of IRRU-14 (Table 2) is not reliable due to its high associated error for both plateau and isochron ages and therefore it is not considered in our study.

3.3. Volume estimates

We have estimated volumes of the Irruputuncu eruptive units and of the whole edifice based on field and GIS measurements (Table 3), complemented with an ASTER Global Digital Elevation Model (ASTER GDEM), with 30 m pixel resolution and accuracy (standard deviation) of 7–14 m, and a topographic coverage with 15-m level curves. For the units deposited over the ignimbritic basement a topographic baseline at 3995 m a.s.l was considered. Minimal volume estimates for each Irruputuncu unit reported (Table 3) were calculated with an estimated error of ~5%, considering exclusively field measurements (altitude) at places were the different units crop out (i.e. only superficial measurements were considered and any, was ignored). The volume of the entire was calculated assuming a simple cone shape (Table 3). Note that, the absence of large scale glacial erosion features suggest very limited erosion of the Irruputuncu volcano, due to the hyper-aridity climate in the Central Andes (e.g. Galli-Olivier, 1967). We have obtained a total minimum volume of ~0.5 km^3 for the superficial units reported in Table 3, and an edifice volume about 4 km^3 (Table 3).

4. Irruputuncu volcano

4.1. General characteristics

In this section we present a detailed stratigraphy of Irruputuncu volcano, summarized in the Fig. 2 (scale 1:50.000), which is based on a detailed geological mapping (scale 1:15.000), rock chemistry (Table 1), ^{40}Ar–^{39}Ar geochronology and K–Ar age data compilation (Table 2), and also report a geochemical evolution of its eruptive products. Irruputuncu volcano products cover an area of 23.861 km^2 (Table 3). We have identified that Irruputuncu volcano was built by two edifices, i) *Irruputuncu I*, a Middle Pleistocene volcano (age ranging between 258.2 ± 48.8 ka and >140 ± 40 ka) characterized by three stages, corresponding to El Pozo pyroclastic flow deposit, Phase I lavas and a debris avalanche deposit (DAD),

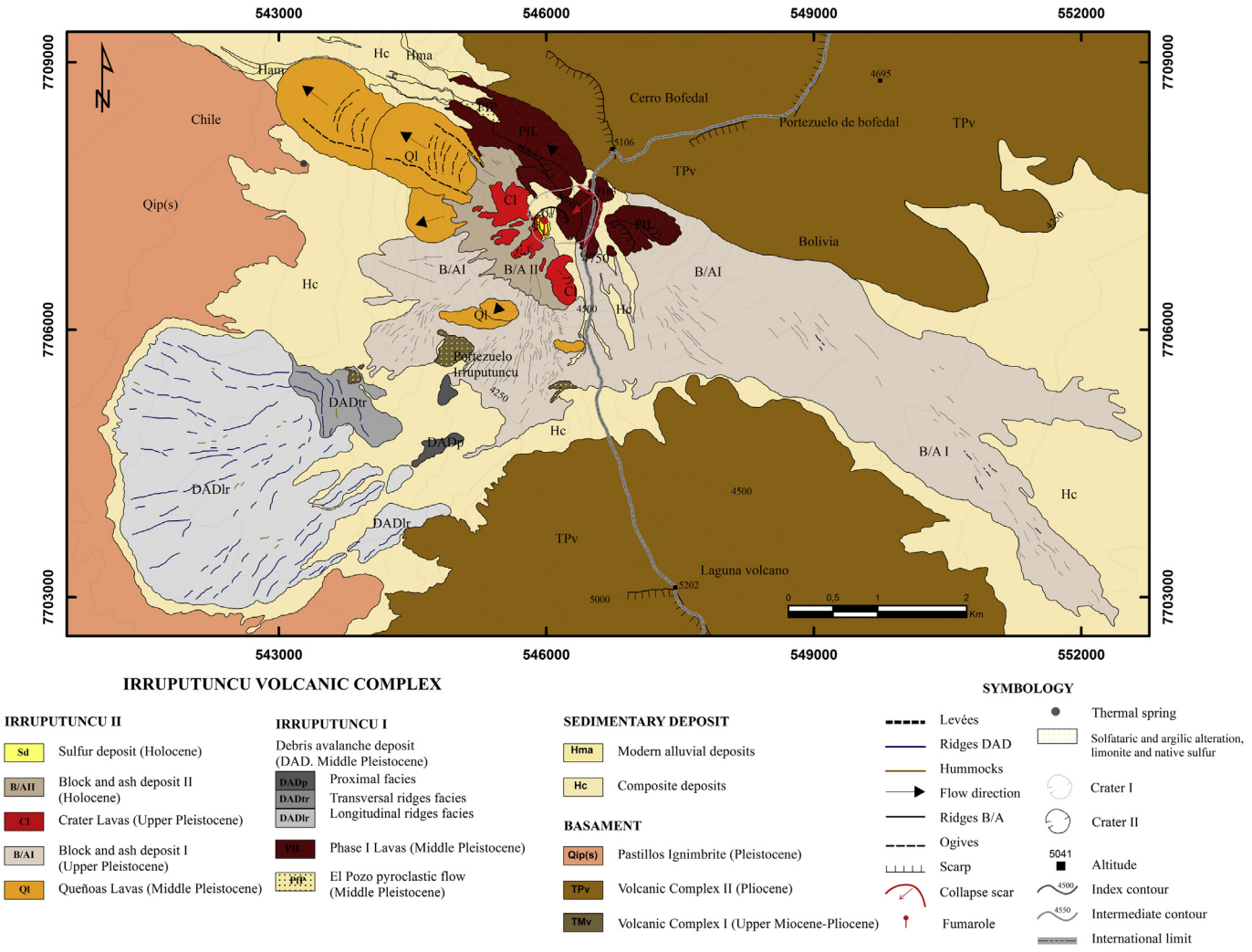

Fig. 2. Geological map of Irruputuncu volcano.

Table 1
Geolocalisation of Irruputuncu samples and major element compositions of whole rocks in wt%.

Sample	UTM coordinates		Stage/unit*	SiO_2	$Al2O_3$	FeO_t**	MgO	CaO	Na_2O	K_2O	TiO_2	MnO	P_2O_5	Total	Reference
	N	E													
IRRU-46A	545450	7708210	$PfP^{(p)}$	63.00	15.88	5.20	2.00	4.19	3.86	2.94	0.64	0.08	0.20	97.99	[1]
IRRU-46B	545450	7708210	$PfP^{(s)}$	59.85	17.07	6.79	2.64	5.49	4.11	2.26	0.80	0.10	0.26	99.37	[1]
IRRU P10a	541559	7705797	$PfP^{(p)}$	62.02	14.80	6.01	2.27	3.78	3.91	3.14	0.73	0.08	0.19	96.93	[1]
IRRU P10b	541559	7705797	$PfP^{(s)}$	61.18	16.44	6.08	2.34	4.90	4.38	2.48	0.72	0.09	0.24	98.85	[1]
IRU-4	544824	7708636	PfP	62.82	16.99	4.84	2.28	5.03	4.25	2.75	0.73	0.09	0.21	99.99	[2], [3]
IRU-98-02	546091	7707593	PIL	60.60	16.60	5.82	2.77	5.13	3.93	2.65	0.88	0.09	0.23	98.70	[2], [3]
IIRU-14	545342	7708350	PIL	61.73	16.14	5.82	2.65	4.77	4.20	2.68	0.77	0.08	0.21	99.05	[1]
IRRU-55	546565	7707510	PIL	61.47	15.99	6.25	2.68	4.54	4.05	2.73	0.81	0.08	0.23	98.83	[1]
IRU-6	545655	7708059	PIL	62.52	16.44	5.41	2.75	4.91	4.23	2.81	0.80	0.08	0.21	100.16	[2], [3]
IRRU-26	543819	7704967	DAD	61.37	16.16	5.97	2.41	4.20	3.71	2.79	0.76	0.07	0.18	97.62	[1]
IRRU-5	543424	7708178	Ql	59.72	16.56	6.24	2.66	5.60	3.79	2.60	0.84	0.06	0.24	98.31	[1]
IRRU-47	544766	7708341	Ql	61.85	16.19	6.20	2.95	5.07	4.11	2.48	0.83	0.08	0.25	100.01	[1]
IRRU-49	544958	7706120	Ql	61.83	16.17	5.98	2.82	4.96	4.12	2.46	0.77	0.08	0.22	99.41	[1]
IRU-98-01	544489	7708250	Ql	62.40	16.40	5.55	2.86	4.96	4.23	2.63	0.80	0.09	0.21	100.13	[2], [3]
IRU-98-05	545237	7707305	Cl	62.50	16.20	5.19	2.28	4.70	4.13	2.75	0.68	0.09	0.19	98.71	[2], [3]
IRRU-50	544761	7706101	B/AI	62.61	15.86	5.89	2.52	4.62	4.19	2.74	0.75	0.08	0.23	99.49	[1]
IRRU-21	546183	7706525	Cl	62.19	15.86	6.10	2.72	4.85	4.07	2.57	0.79	0.08	0.23	99.46	[1]
IRRU-18	546059	7707202	Cl	62.36	16.04	5.86	2.58	4.65	3.98	2.75	0.76	0.08	0.23	99.29	[1]
IRU-98-04	545695	7707305	Cl	62.10	16.00	5.12	2.52	4.68	4.09	2.73	0.74	0.08	0.20	98.26	[2], [3]
IRU-98-09	545789	7707516	Cl	62.90	15.60	4.28	1.81	3.97	3.68	3.07	0.59	0.07	0.17	96.14	[2], [3]
IRRU-60	545858	7706702	B/AII	62.06	16.09	6.21	2.74	4.81	4.21	2.64	0.78	0.08	0.20	99.82	[1]
IRU-98-08	546007	7707305	Sd	64.60	15.80	4.46	1.97	4.02	4.07	3.09	0.63	0.07	0.18	98.89	[2], [3]
IRU-98-06	545955	7707305	Sd	62.40	15.80	5.40	2.6	4.48	4.02	2.74	0.80	0.08	0.18	98.50	[2], [3]
IRU-1d	544814	7708780	Hc	59.74	17.71	6.52	2.47	5.65	3.66	2.32	0.83	0.10	0.34	99.34	[2], [3]
IRU-1b	544762	7708847	Hc	61.72	17.58	5.24	2.49	5.24	4.10	2.51	0.78	0.09	0.22	99.97	[2], [3]
IRU-1a	544626	7708869	Hc	63.92	15.21	4.54	1.93	3.80	3.66	3.42	0.65	0.08	0.17	97.38	[2], [3]
IRU-1c	544835	7708802	Hc	60.33	17.85	5.80	2.72	5.73	4.16	2.20	0.85	0.10	0.24	99.98	[2], [3]

[1] This work.
[2] Mamani et al. (2008; 2010).
[3] Wörner et al. (1992).
* See Fig. 2 for description of the units.
** FeO_t as FeO.
(p): pumice.
(s): scoria.

that resulted from flank collapse, which finished the active period of this first edifice; ii) *Irruputuncu II*, a Middle Pleistocene to Holocene volcano (<140 ± 40 ka-recent) built in the southwestern flank of Irruputuncu I collapsed edifice, is characterized by 4 stages (Queñoas lava flows, Block and ash deposit I, Crater lavas and, Block and ash deposit II).

4.2. Geochemical evolution

Whole rocks of the Irruputuncu volcano have almost identical mineral and chemical compositions and are characterized by andesitic, trachy-andesitic and dacitic lavas (with a minor pyroclastic flow deposit), with plagioclase > biotite > hornblende > pyroxene as main mineral assemblage. Geochemical data (Fig. 3a–b and Table 1) indicate that Irruputuncu magmas are typical subduction type high-K calcalkaline magmas, with restricted SiO_2 and K_2O contents that range from 59.7 to 63.0 wt%, and 2.26 to 3.14 wt%, respectively.

The concentration of K_2O increases with the enrichment of SiO_2 (Fig. 3c), whereas, compatible elements such as Ti, P, Fe, Mg, Al and

Table 2
Geochronological data of Irruputuncu volcano. Bold corresponds to the isochron age with lower MSWD.

Sample	UTM coordinates		Unit	Sample description	Method	Age plateau analysis**		Inverse isochron analysis**		Reference
	E	N				Age (ky)	MSWD	Age ± 2σ (ka)	MSWD	
IRRU-21	546190	7706730	Cl	Lava block	Ar–Ar (groundmass)	**55.9 ± 26.8**	3.97	32.0 ± 13.5	3.96	This work
IRRU-P10	541306	7704614	DAD	Pumice beneath the DAD	Ar–Ar (biotite)	**109.8 ± 79.1**	0.75	180.9 ± 137.6	0.84	This work
IRRU 46-A	545450	7708210	PfP	Pumice	Ar–Ar (biotite)	173.3 ± 11.6	1.75	**258.2 ± 48.8**	0.36	This work
IRRU-14	545620	7708220	PIL	Flow NW of cone	Ar–Ar (groundmass)	**10.2 ± 21.1***	0.26	7.7 ± 6.5	0.27	This work
n/n	545858	7706702	B/AII		^{14}C	**1.57 ± 0.9**	-	-	-	Stern et al., 2007
IRRU11	544830	7708535	Ql	Younger upper flow on W slope	K–Ar (biotite)	**140 ± 40**	–	–	–	Wörner et al., 2000
IRRU10	544540	7708228	Ql	Lower flow on W base of cone	K–Ar (biotite)	**450 ± 400***	–	–	–	Wörner et al., 2000
IRU15	539901	7703628	Qip(s).Upper member	Ignimbrite on Pampa Irruputuncu	K–Ar (biotite)	**320 ± 25**	–	–	–	Wörner et al., 2000
IRRU17	537715	7695794	Qip(s). Lower member		K–Ar (biotite)	**750 ± 20**	–	–	–	Vergara and Thomas, 1984

* not reliable (see text for discussion).
** preferred ages in bold (see text for discussion).

Ca show decrease in concentration with the increase of SiO_2 content (Fig. 3d and f–j). No trend is observed for Na (Fig. 3e). Furthermore, a decrease of the Anorthite content of the plagioclases is observed with increase of the silica content (Fig. 4a), which indicate differentiation in the magma chamber of Irruputuncu volcano. Additionally, the positive correlation of CaO with MgO (Fig. 4b), indicates the removal of these components from a liquid due to the co-crystallization of plagioclase and clinopyroxene (Rollison, 1993).

4.3. Irruputuncu I

4.3.1. El Pozo pyroclastic flow deposit (PfP)

El Pozo deposit is located in the northwestern side of volcano (Fig. 2), and covers an area of ~0.02 km^2, corresponding to a minimum volume of ~0.001 km^3 (Table 3). This deposit resulted from small pyroclastic flows that were emitted from Crater II to the northwestern side of the volcano (an exclusive original outcrop is preserved and extends over ~0.35 km). It is the oldest Irruputuncu unit that we have identified. We acknowledge that El Pozo deposit might have been generated by an older edifice that has been eroded or is now hidden; however, we consider this unit has part of the Irruputuncu history, because field observation show that El Pozo unit underlies the Phase I lavas and the debris avalanche deposit (Fig. 5a) described in the next section, which provides constraints on the relative time emplacement of these units. The age of El Pozo deposit has been determined at 258.2 ± 48.8 ka (Ar–Ar method on biotites in pumice, Table 2), while a sample at the base of the debris avalanche deposit gave an age of 109 ± 79 ka. The youngest age of the sample beneath the avalanche was possibly due to alteration. Taking into account the low error of the first age of the non-remobilized deposit, we consider that 258.2 ± 48.8 ka is the most reliable age for the El Pozo unit.

The El Pozo unit has a thickness of ca. 50 m and was formed by the accumulation of several pumice flow deposits whose thicknesses vary between 90 and 140 cm. This deposit is glassy pumice-rich and clast-supported, has a fine-grained ash matrix (5% vol.) and is poorly sorted. It contains coarse pumices (65% vol., size <50 cm), scorias (8% vol., size <7 cm), mixed scoria-pumice fragments (10% vol., size of 0.5–20 cm, Fig. 5c), lithic clasts (7% vol., size of 1–30 cm) and free biotite crystals (5% vol., 2 mm diameter). The lithics are sub-angular to angular and there are at least three populations of clasts, all with evidence of Fe alteration (Fig. 5d). Both the pumices and scoria are sub-rounded to sub-angular. The different flow units present reverse size grading typical of dense granular flows.

The El Pozo deposit has a bulk chemical composition that varies from trachy-andesitic to trachy-dacitic (62–63 wt% SiO_2, Table 1, Fig. 3). It contains crystals of plagioclase (~10% vol. An_{47-54}), hornblende (~5% vol.) and biotite (~8% vol.) in a matrix (~77% vol.) of abundant glass, and plagioclase–amphibole microlites. Some biotite and plagioclase crystals present disequilibrium textures (opaque minerals in the edges and sieve texture, respectively). The scoria fragments (59.8–61.2 wt% SiO_2, Table 1) contain crystals of plagioclase (3% vol.), amphibole (1% vol.) and biotites (1% vol.) in a matrix of glass, plagioclase, amphibole and biotite minerals. The mixed scoria-pumice clasts (Fig. 5c) contain plagioclase (~15% vol.), quartz (~10% vol.), hornblende (~3% vol.) and biotite (~7% vol.) in a glassy matrix (~65% vol.).

4.4. Phase I lavas (PIL)

This unit includes lava flows and domes that constitute the older Irruputuncu edifice (Irruputuncu I; Fig. 2). These are blocky lavas of trachy-andesitic composition (60.60–62.52 wt% SiO_2; Table 1) with plagioclase and biotite as main minerals phases. Lava flows are located in the northern and eastern sides of the volcano, while at least one lava dome was recognized in the north eastern side of Crater I, the older and northeasternmost crater. The lava dome and flows were emitted to the northwest, northeast and east–southeast directions from Crater I, overlaying the regional basement (corresponding mainly to Pastillos Ignimbrite), and to the El Pozo pyroclastic flow deposit, whilst they underlie partially by the block-and-ash flow deposit I (Fig. 5a–c). Despite the lava flows are poorly preserved, they show smooth surfaces affected by alluvial erosion as well as, primary structures (hereafter called ogives), that are oriented perpendicular to the emplacement direction and that are easily recognized in the east–southeast flows. Lava flow thickness varies from 35 to 113 m. Phase I lavas cover an area of 1.692 km^2 and have a minimum volume of ~0.097 km^3 (Table 3). No reliable age was obtained for this unit (10.2 ± 21.1 ka from $^{40}Ar-^{39}Ar$ in groundmass, Table 2). Therefore, only stratigraphic relations can be used to estimate the age of Phase I Lavas, which is ~258–140 ka (Middle Pleistocene, Table 2) based on ages of the El Pozo and Queñoas units.

The Phase I lavas show porphyritic, disequilibrium, hypocrystalline textures. Phenocrysts are plagioclases (~20% vol. An_{47-57}) with reabsorption edges and sieve texture (Fig. 7a), biotites (~9% vol.) with glomeroporphyritic textures and occasional pyroxenes at the edge in disequilibrium texture, and hornblendes (~6% vol.). The groundmass (~65% vol.) presents hyalopilitic texture and consists mainly of glass, plagioclase microlites, biotites, hornblendes and opaque minerals.

4.5. Debris avalanche deposit (DAD)

The debris avalanche deposit (DAD) is a fan-shaped, radial front deposit on top of the Pastillos ignimbrite basement (Figs. 2 and 8a). It extends ~6.3 km southwest from the Crater I, covers an area of ~7.05 km^2, has a maximum thickness of ~10 m and a minimum volume of ~0.071 km^3 (Table 3). This deposit is homogeneous and shows scarce alluvial erosion, except in the distal zone.

The DAD contains blocks of andesitic to trachy-andesitic composition similar to the phase I lavas (61.37 wt% SiO_2, Table 1. Fig. 3). The blocks have a size up to 6 m, occasionally present jigsaw structures and impact marks (Fig. 8b–c) and are embedded in a ash-

Table 3
Estimated area and volume of Irruputuncu units.

Stage	Irruputuncu I			Irruputuncu II					Sedimentary deposit
Unit	PfP	PIL	DAD*	Ql	B/AI	Cl	B/AII	Sd	
Area (km^2)	0.02	1.692	7.051	2.461	11.333	0.492	0.801	0.011	3.911
Volume (km^3)[a]	0.001	0.097	0.071	0.309	0.023	0.042	0.001		0.002
Cumulated volume (Km^3)	0.169			0.375					0.002

*: DADp (0.12 km^2); DADrt (0.76 km^2); DADlr (6.85 km^2).
[a] : Minimum volume calculated from field measurements.

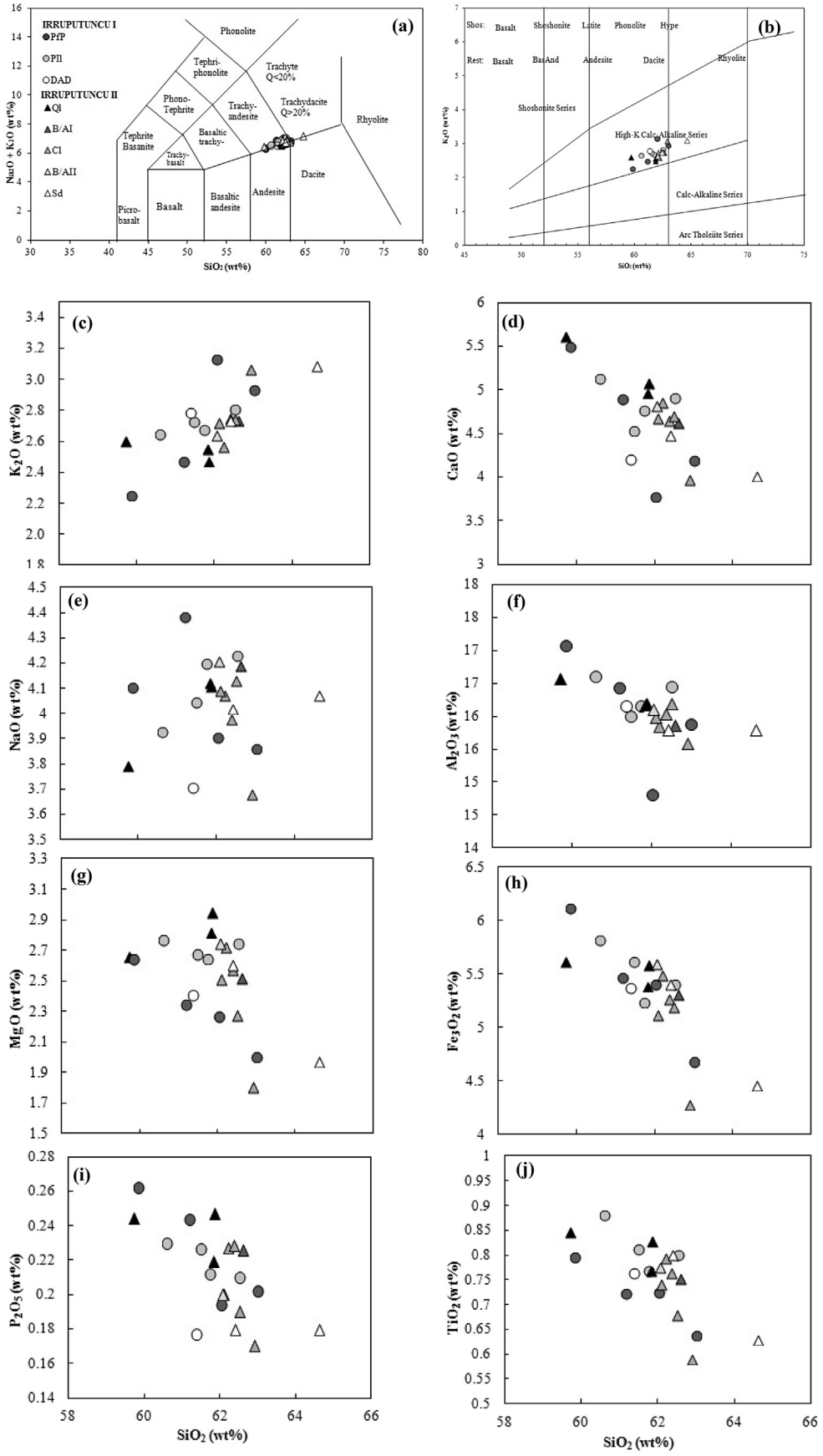

Fig. 3. Geochemical diagrams of whole rocks chemistry of Irruputuncu units. (a) Whole-rock geochemistry TAS diagram. (b) K_2O vs SiO_2 diagram. (c–j) Major elements vs SiO_2.

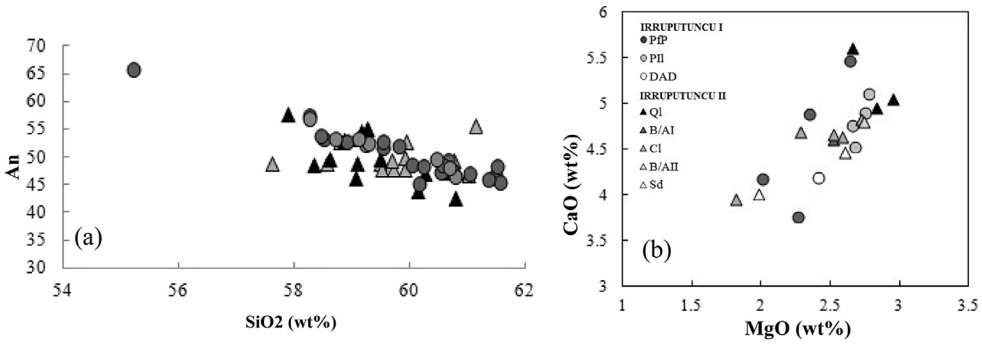

Fig. 4. (a) Anorthite composition vs SiO_2. (b) Variation of CaO with MgO of rocks of Irruputuncu volcano.

lapilli size matrix. Field observations suggest that the DAD resulted from the collapse of the SW flank of the Irruputuncu I volcanic edifice. According to the distribution of large-scale deposit structures, such as hummocks and ridges (Fig. 8a), and to the characteristics of the individual blocks (e.g. jigsaw fractures), the DAD unit has been divided in three sub-units as described below (Fig. 8a).

No radiometric data exists for this deposit and only relative age can be inferred from stratigraphic relations. Considering that the DAD is younger than the Phase I lavas and older than the Queñoas lava flow, this suggest that the DAD is older than 140 ± 40 ka (Table 3) and has a Middle Pleistocene age.

4.6. Proximal facies (DADp)

This proximal sub-unit covers an area of ~0.1076 km^2. The deposit contains lava blocks of andesitic composition, which does not exceed 2 m in diameter and are subangular with well-developed jigsaw structures. No structures such as hummocks and ridges can be observed in this sub-unit (Fig. 8a). The rocks present porphyritic, hypocrystalline, glomeroporphyritic, poikilitic and intersertal textures. They contain phenocrysts of plagioclase (~20% vol.) typically with reabsorption rims, biotite (~10% vol.), brown hornblende and oxyhorblende (~4% vol., sometimes with disequilibrium edge being replaced by pyroxene), and quartz (~1% vol.). The groundmass (~65% vol.) consists of glass, microlites of plagioclase, pyroxene, and biotites.

4.7. Transversal ridge facies (DADtr)

This proximal to intermediate sub-unit located in the middle part of the DAD covers an area of ~0.536 km^2. It is characterized by ridges <700 m in length that are oriented N–S – NW–S, transverse to the inferred avalanche propagation trend (Fig. 8a). The DADtr unit contains blocks of andesitic composition (61.37 wt% SiO_2, Table 1, Fig. 3). Most of the blocks show jigsaw structures. The andesitic lava blocks present hypocrystalline and porphyritic textures. Their phenocrysts are constituted by plagioclases (~15% vol.) with zonation and reabsorption features, biotites (~8% vol.) and hornblende (~3% vol.) The groundmass (~74% vol.) contains glass, microlites of plagioclase, hornblendes, biotites and opaque

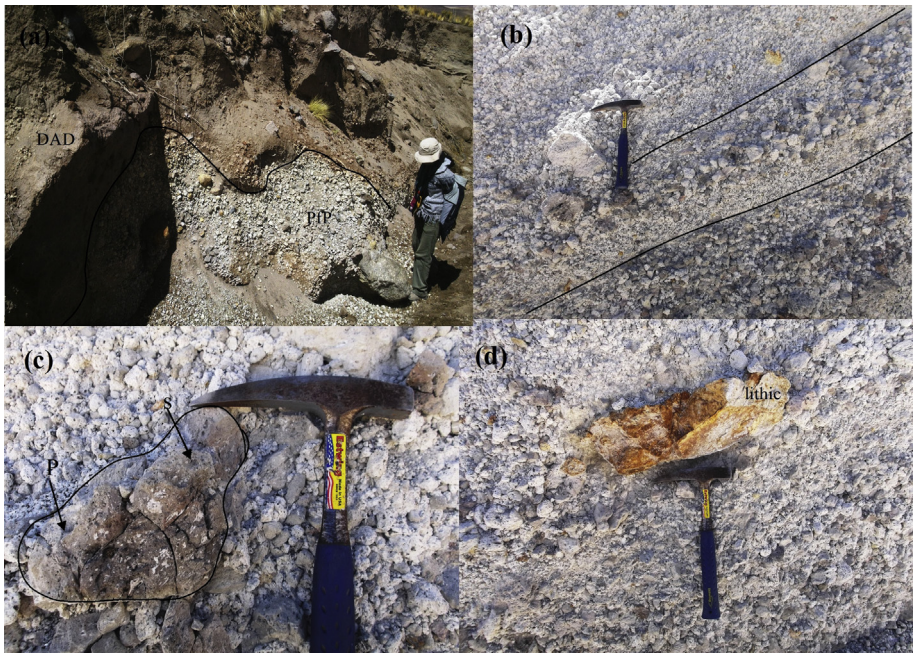

Fig. 5. Field photograph of El Pozo pyroclastic flow deposit. (a) El Pozo deposit (PfP) beneath the debris avalanche deposit (DAD). (b) Pumice flow deposit units showing reverse size grading of pumices and scoria clasts. (c) Large pumice (P) and scoria (S) clasts with evidence of magma mingling. (d) Altered lithic clast.

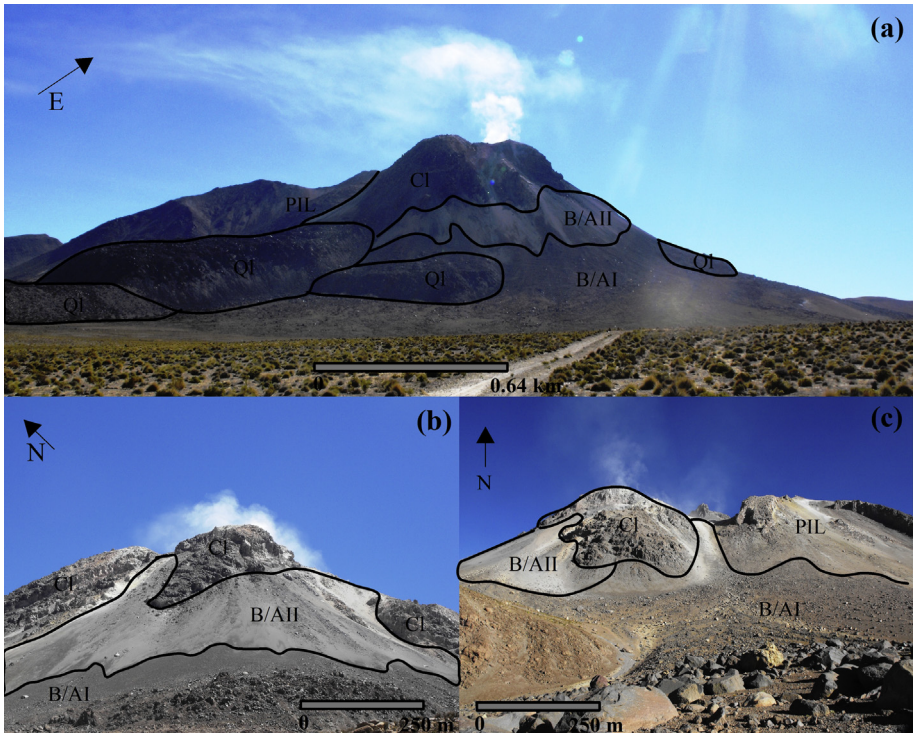

Fig. 6. Panoramic view of Irruputuncu units. (a–c) Contacts between Phase I lava (PIL) and Crater lava flows (Cl), with block-and-ash flow deposits I and II (B/AI and B/AII) covering the Queñoas lava flows (Ql) and Crater lavas.

minerals.

4.8. Longitudinal ridges facies (DADlr)

This is the most distal facies of the debris avalanche deposit, which has a fan-shaped radial front. It is the most extended sub-unit as it covers an area of ~6.439 km^2. It rests on the Pastillos Ignimbrite (Fig. 2) and covers partially the Volcano-Group II (TPv in Fig. 2) unit to the SW. The deposit morphology is dominated by hummocks and ridges (oriented mainly SW–NE) longitudinal to the inferred flow trend, but with some radiating pattern. The ridges can be up to ~1 km long and their height is up to 2 m. Most blocks present impact marks and jigsaw structure.

This sub-unit is mainly composed by andesitic lava blocks of size <6 m, which are occasionally partially altered. The rocks present porphyritic, hypocrystalline and poikilitic textures. The main minerals are plagioclases (~20% vol.) with reabsorption at their edges, biotites (~10% vol.) scattered or in clusters (glomeroporphyritic texture), brown hornblendes (~2% vol.) replaced by pyroxenes at their edges (disequilibrium texture), and orthopyroxene (~2% vol.) in clusters (glomeroporphyritic texture). The groundmass (~66% vol.) is constituted by glass, microlites of plagioclase, hornblendes and opaque minerals.

4.9. Irruputuncu II

4.9.1. Queñoas Lavas flows (Ql)

This unit is formed by six blocky lava flows located NW, W and SW of Irruputuncu II edifice. The flows extend from Crater II (Figs. 2 and 9a) to a distance of 1.22–3.4 km, they cover an area of ~2.461 km^2 and have a minimum volume of ~0.329 km^3 (Table 3). The W, SW and S lavas have thicknesses of ~23–95 m, while the NW lavas are ~117–180 m-thick. The lava flows are of andeistic to trachy-andesitic composition (59.7–62.40 wt% SiO_2; Table 1, Fig. 3a, see also Wörner et al., 1992 and Mamani et al., 2010) and contain plagioclases and biotites as phenocrysts. The Queñoas lavas were

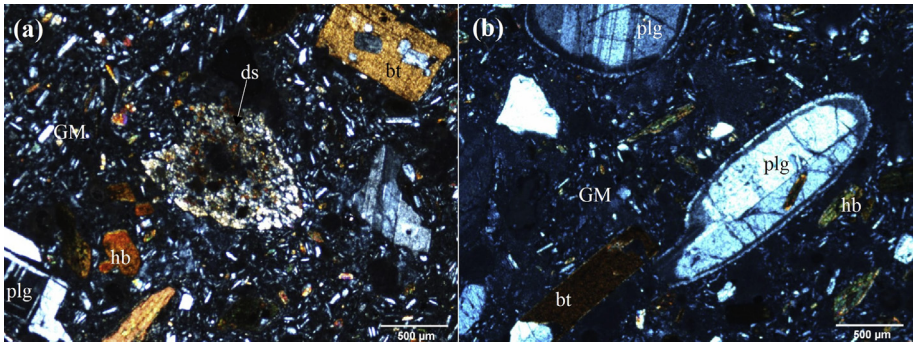

Fig. 7. (a) Photomicrography of Phase I lavas showing biotite (bt) and mafic minerals with disequilibrium texture (ds) in a groundmass (GM) of plagioclase microlites. (b) Photomicrography of Crater lava flows showing plagioclases (plg) with resorption and biotites (bt) in a hypocristalline groundmass (GM).

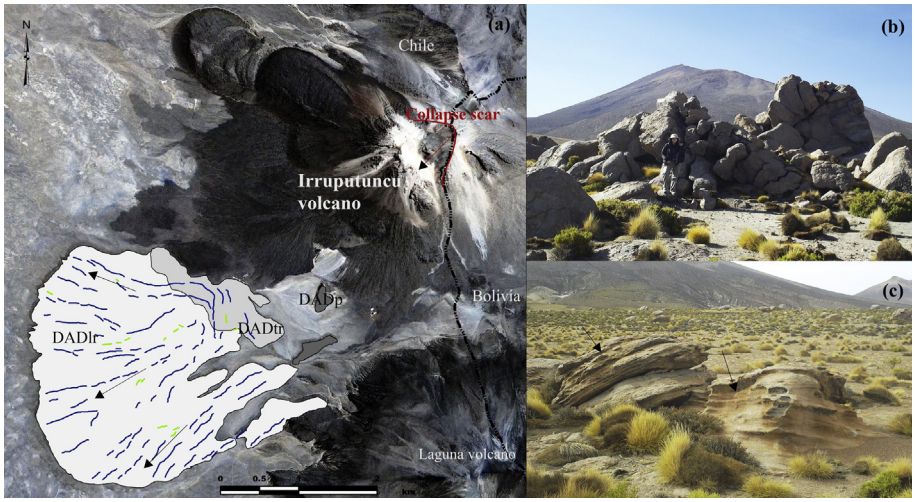

Fig. 8. (a) Satellite image showing the debris avalanche deposit (DAD). The black arrows indicate the flow direction; blue lines indicate ridges and green lines represent hummocks. (b) Blocks with jigsaw structure. (c) Impact marks on blocks (shown by arrows). (For interpretation of the references to color in this figure legend, the reader is referred to the web version of this article.)

emplaced partially over an older edifice (Volcanic Group I) in the southwestern flank of the volcano and they overlie the Pastillos Ignimbrite in the NW part of the study area. This unit is partially covered by the block-and-ash flow deposit II near the summit, while they are partially surrounded by the block-and-ash flow deposit I to the south (Fig. 6a). The lava flows are well preserved. The west, southwest and south flows, while northwest flows show lobate surface structures, while the northwest flow presents lateral levees and ogives structures (Fig. 9a). Two ages of 140 ± 40 ka and 450 ± 400 ka (Middle Pleistocene) were determined by Wörner et al. (2000) for the Queñoas Lavas flows (K–Ar method on biotite; see Table 2). The latter age is not reliable as it has a large error due to the small amount of radiogenic Ar in the biotites analyzed, and it is not considered in this study.

The rocks present hypocrystalline, porphyritic, glomeroporphyritic, poikilitic, intersertal and disequilibrium textures. The phenocrysts are mainly plagioclase (~13% vol. An_{42-58}) with reabsorption rims and sieve texture (Fig. 9b), biotites (~6% vol.) and hornblendes (~3% vol.) that form clusters and show evidence of disequilibrium at their edges (Fig. 9c), clinopyroxenes (~3% vol.) and orthopyroxenes (~2% vol.) either scattered or forming clusters. The groundmass (~73% vol.) is composed of glass, microlites of plagioclase, biotite, pyroxenes, hornblende and opaque minerals.

4.10. Block and ash flow deposit I (B/AI)

This pyroclastic flow deposit is located on the W, SW and SE flanks of the volcano, constituted exclusively by a monotonous trachy-andesitic composition (62.61 wt% SiO_2; mineral assemblage plagioclase > biotite; Table 1). The deposit has a mean thickness of 2 m, covers an area of ~11.333 km^2, and has a minimum volume of ~0.023 km^3 (Table 3). It overlies the Queñoas lavas and the Phase I Lavas units (Fig. 6b and 10a) and is partially covered by the block-and-ash II deposit described below. One of most notable characteristics of this deposit are very well developed surface ridge structures of length up to ~600 m (Fig. 2). To the east, the flows were channeled in the Volcanic Group II unit (TPv in Fig. 2) and were highly mobile since they traveled up to ~7.1 km from their source on slopes as low as 11° in distal areas. The block and ash deposit I is massive, matrix-supported and very poorly sorted deposit. It contains large angular blocks of size <3 m in a matrix of ash-lapilli size clasts (Fig. 10b). Sporadic blocks of size up to 15 m can be found. The large clasts are subangular-to-angular.

The rocks present porphyritic, hypocrystalline, and disequilibrium textures. The phenocrysts have the following characteristics: plagioclases (~18% vol.) show reabsorption textures (Fig. 10c) that occasionally contain hornblende crystals (poikilitic texture), hornblendes (~4% vol.) form clusters and show disequilibrium texture, biotites (~10% vol.) may contain plagioclase crystals, while small amounts of clinopyroxenes and orthopyroxenes (~3% vol.) are also present. The groundmass (~65% vol.) contains glass, microlites of plagioclase, amphibole, biotite and opaque minerals. Isolated quartz crystals with clinopyroxene in their edges (coronitic texture) could be interpreted as xenocrysts (Fig. 10d).

According to the chemistry of the blocks described above, we interpret the block-and-ash flow deposit I as the result of the collapse of one or several lava domes whose remnant could correspond to parts of the Queñoas lavas unit. We propose that the age of this deposit is between 55.9 ka and 140 ka (Table 2) based on ages of the Queñoas and Crater lavas.

4.11. Crater lavas (Cl)

This units consists of lavas domes and small blochy lava flows of trachy-andesitic composition 62.2% SiO_2, (see also Wörner et al., 1992, and Mamani et al., 2008, 2010; Table 2, Fig. 3a). There are at least seven small flows of length of 0.54–0.94 km and thickness of 68–107 m and that present weakly developed surface ogive structures. This unit is distributed in the SW upper parts of the volcanic edifice and was emitted from or nearby Crater II (Fig. 2). It covers an area of ~0.492 km^2 and has a minimum volume of ~0.042 km^3 (Table 3). The lavas delimit the currently active crater, are covered partially by the block-and-ash flow deposit II (Fig. 6a–c), are locally in contact with Phase I lavas (Fig. 6a), and cover to Queñoas lavas stage. We obtained an age of 55.9 ± 26.8 ka based on the $^{40}Ar/^{39}Ar$ method on groundmass (Table 2).

The Crater lavas present porphyritic, hypocrystalline, poikilitic and disequilibrium textures. The phenocrysts are plagioclases (~18% vol. An_{44-54}) with sieve texture, biotites with skeletal texture (~8% vol.), hornblendes (~4% vol.) that sometimes, both mafic minerals show disequilibrium texture with pyroxenes crystals at their edge, and clino and orthopyroxene (~2% vol.) with

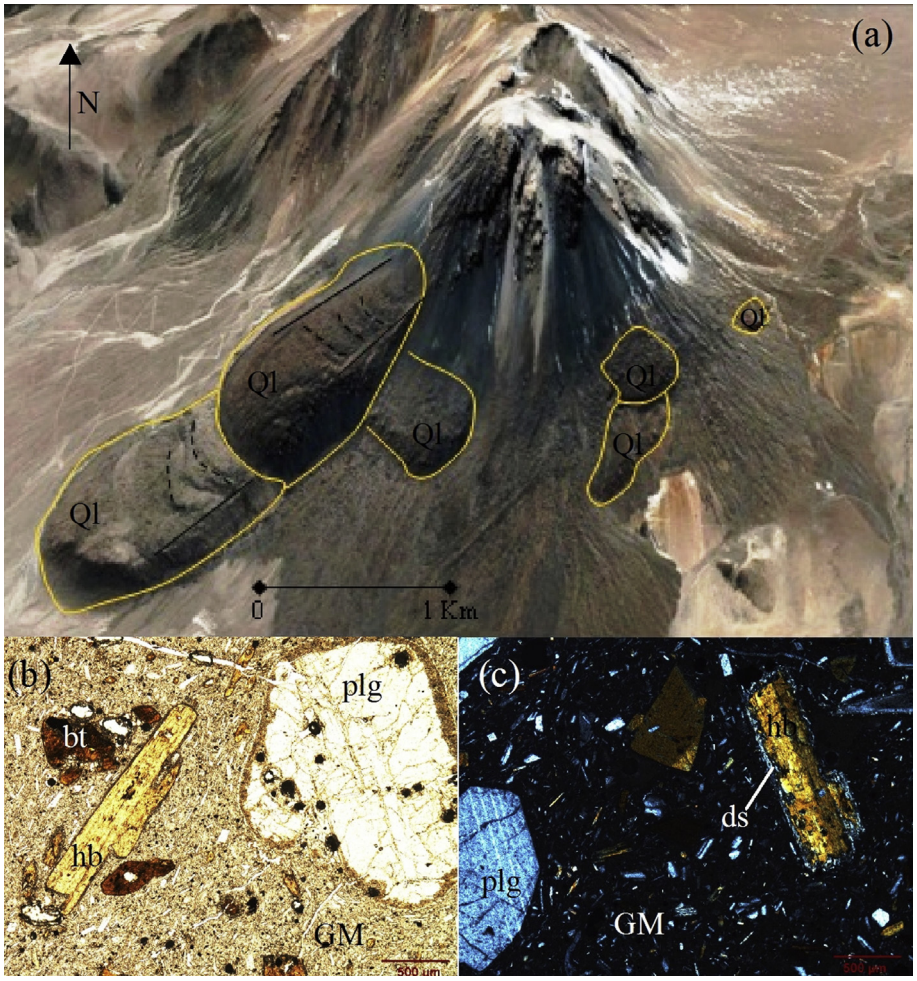

Fig. 9. (a) Satellite image showing the Queñoas lava flow unit (orange line), with lateral levées (solid line) and concentric ridge structure (ogives in dashed lines). (b) Photomicrography showing phenocrysts of plagioclase (plg) with disequilibrium texture, hornblende (hb) and biotites (bt) in a hypocristalline groundmass (GM). (c) Photomicrography showing phenocrysts of hornblende (hb), with disequilibrium texture (ds), and of plagioclase (plg) in a hypocristalline groundmass (GM). (For interpretation of the references to color in this figure legend, the reader is referred to the web version of this article.)

disequilibrium texture outlined by hornblende. The groundmass (~68% vol.) consists of glass, and microlites of plagioclases, biotites, hornblendes, clinopyroxenes, and opaque minerals.

4.12. Block and ash flow deposit II (BA/II)

This block-and-ash flow deposit located on the northwest, west and southwest flank of the volcano has an age of 1.57 ± 0.9 ka (^{14}C method, Stern et al., 2007, Table 2). It covers an area of ~0.801 km^2 and has a minimum volume of ~0.001 km^3 (Table 3). This unit was formed by collapse of lava domes located initially in or nearby Crater II or the active crater. It extends for 1.1 km from the active crater and overlies partially the block-and-ash flow deposit I as well as the Queñoas and Crater lavas units (Fig. 2 and Fig. 6a–c, note that the deposit is partially covered by recent screes). This deposit has poorly developed ridge structures. It is massive and poorly sorted and is constituted by subangular to angular blocks in an abundant dark gray matrix of lapilli-ash sixe clasts. Most blocks are 0.5 min diameter, but some blocks of size up to ~1 m are found in highest part of volcano near the active crater.

This deposit is of trachy-andesitic composition (62.06 wt% SiO_2, Table 1). The rocks present a porphyritic texture, with phenocrysts of plagioclase (~15% vol.) and biotites (~8% vol.) while the groundmass (~77% vol.) consists of glass, and microlites of plagioclase and mafic minerals.

4.13. Sulfur deposits (Sd)

Active sulfur deposits are found in the active Irruputuncu crater that has a diameter that varies from ~40 to ~85 m (Fig. 11a) and they cover an area of ~0.011 km^2 (Fig. 2, Table 3). Small overlapping sulfur flows have a maximum length of 2 m, a width of 10–30 cm and a thickness up to 5 cm. They present pahoehoe-type morphology with poorly developed lateral levees (Aguilera, 2008). The color of these sulfur deposits is mainly yellow, although near to the fumarolic centrers it may be orange, red, gray or black depending on the emission temperature of the fumaroles (Naranjo, 1985, Fig. 11b).

4.14. Sedimentary deposits (Hc and Hma)

Recent sedimentary units consist of alluvial, colluvial and eolian deposits. Alluvial and colluvial deposits are unconsolidated to poorly consolidated, and they contain fragments whose size varies from gravel to sand and that are derived from Irruputuncu I and II edifices (Hc unit; Fig. 2). Alluvial deposits are found in active

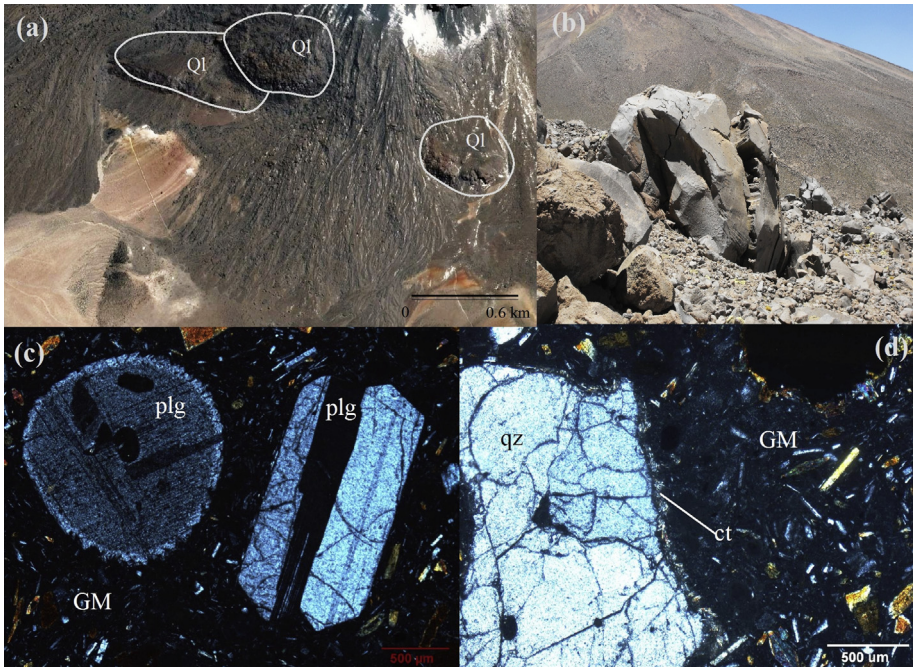

Fig. 10. Block-and-ash flow deposit I (B/AI). (a) Satellite image showing the B/AI covering partially to Queñoas lava unit (Ql). (b) Large fractured lava blocks. View is to the east. (c) Photomicrography showing xenocrysts (round) and phenocrysts of plagioclase (plg) with disequilibrium texture in a hypocristalline groundmass (GM). (d) Photomicrography showing xenocrysts of quartz (qz) with coronitic texture (ct).

channels re-activated by sporadic summer rains (Hma unit; Fig. 2). They contain gravel to sand size fragments that correspond mainly to andesitic lava fragments, pumice, and biotite-quartz crystals, and they show fine lamination and rare cross-laminations. Colluvial deposits are frequently found on the upper parts of Irruputuncu II southern flank and are constituted by abundant altered rock fragments originated in the active crater area. Fine-sand eolian dunes of height <1 m are found frequently in the southern zone of the study area, 1 km east to the DAD longitudinal ridge facies.

It is interesting to note that a little glacial age occurred in Central Andes between ~15 ka and ~11 ka (e.g. Grosjean et al., 1995), which promoted glacial erosion on several volcanic edifices (e.g. de Silva and Francis, 1991). However, there is no evidence of such erosion, like U-shape valleys and moraine deposit, on the Irruputuncu volcano. In consequence, it appears that the Irruputuncu volcano did not host glaciers.

5. Discussion

5.1. Volcanic evolution

In this paper we provide the first detailed geological map of Irruputuncu volcano and reconstruct the main stages of the eruptive history of this edifice, as summarized in Fig. 12. The Irruputuncu edifice was built during two main stages that we named Irruputuncu I and Irruputuncu II.

Irruputuncu I began at least ~258 ± 49 ka ago, assuming that the El Pozo unit is part of Irruputuncu eruptive history. Texture of clasts in the El Pozo deposits suggests mingling of trachy-andesitic magmas, one being slightly more evolved (pumice fragments, 62–63 wt% SiO_2) than the other (scoria fragments, 59.8–61.18 wt% SiO_2), possibly through injection of a hotter and less evolved magma in a pre-existent colder and more evolved magma. Such a mechanism may have triggered the El Pozo eruption, as proposed for other explosive eruptions in the Central Andes and elsewhere (e.g. Matthews et al., 1999). Then, eruptive activity turned effusive. Trachy-andesitic Phase I lava flows were emitted at ~258–140 ka from the Crater I, which was hosted in the summit of the original Irruputuncu I. Interestingly, this magma has a composition similar to the less evolved component of El Pozo unit (cf. scoria), which suggests that both units originated from the same magmatic system.

The volcanic edifice that grew during this first stage became unstable and big enough to experience the collapse of its western flank, as shown by the debris avalanche deposits (DAD) that extend to at least 6.3 km from the volcano and cover an area of ~7.1 km^2. This event marked the end of Irruputuncu I. A notable feature of the DAD unit is the transition from proximal deposits without clear surface structures, to intermediate deposits with transversal ridges and finally proximal deposits with longitudinal ridges and hummocks. There is no evidence to relate the flank collapse to magmatic intrusion processes, and the absence of altered blocks in the DAD deposits suggests that the edifice was not significantly physically altered. In consequence, sector collapse could have been caused by edifice asymmetry and/or by the overstepping of the southwest flank that might have been triggered by overloading of the volcano and/or an earthquake.

Irruputuncu II stage began at 140 ± 40 ka (Wörner et al., 2000) with the formation of the new crater (Crater II) and the emission of the Queñoas lava flows, which is the most voluminous Irruputuncu II effusive unit (~0.3 km^3). Queñoas lavas probably filled the scar of Irruputuncu I edifice created by the debris avalanche and they also formed thick (>100 m) flows of limited lateral extension, possibly because of a high magma viscosity and/or low eruptive rate. This was followed by collapse of lava domes(s) built on top of the edifice as shown by the block-and-ash flow deposit I. These flows propagated mainly to the East on moderate distal slopes (~11°) and had a fairly long run-out distance of about ~7.1 km. Such high flow mobility could have resulted from large-volume and/or sustained dome collapse (e.g. Calder et al., 1999). The eruptive activity continued with an effusive stage (Crater lava unit) at 55.9 ± 26.8 ka that formed the present crater and probably also lava domes. The

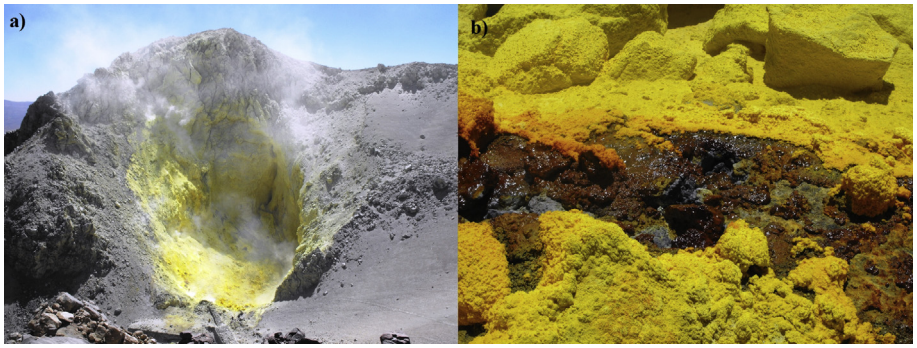

Fig. 11. (a) Irruputuncu volcano active crater with abundant fumarolic activity and yellow sulfur deposits. The maximum crater width is 85 m. (b) Photograph showing sulfur deposits in the fumarolic field. (For interpretation of the references to color in this figure legend, the reader is referred to the web version of this article.)

last activity corresponds to the collapse of lava domes, which generated the small block-and-ash flow deposit II 1.57 ± 0.9 ka ago. Present Irruputuncu activity consists of deposition of sulfur in the active crate and permanent fumarolic activity.

5.2. Magmatic processes

The Irruputuncu eruptive products described in this study are of andesitic to trachy-andesitic composition and belong to the high-K calc-alkaline series (2.56–2.79 wt% K_2O; 59.7–63 wt.% SiO_2) typical of active volcanoes of the Central Andes (e.g. Parinacota, Wörner et al., 1988; Tata Sabaya, de Silva et al., 1994; Ollagüe, Feeley and Davidson, 1994). Incompatible and compatible elements show a normal behavior with respect to the silica content, as observed in other volcanic centers of the CVZ (e.g. Lastarria, Llullaillaco, Parinacota, Lascar), and we suggest that the magmatic evolution was controlled mainly by fractional crystallization. The behavior of CaO and MgO indicates co-crystallization of plagioclase and

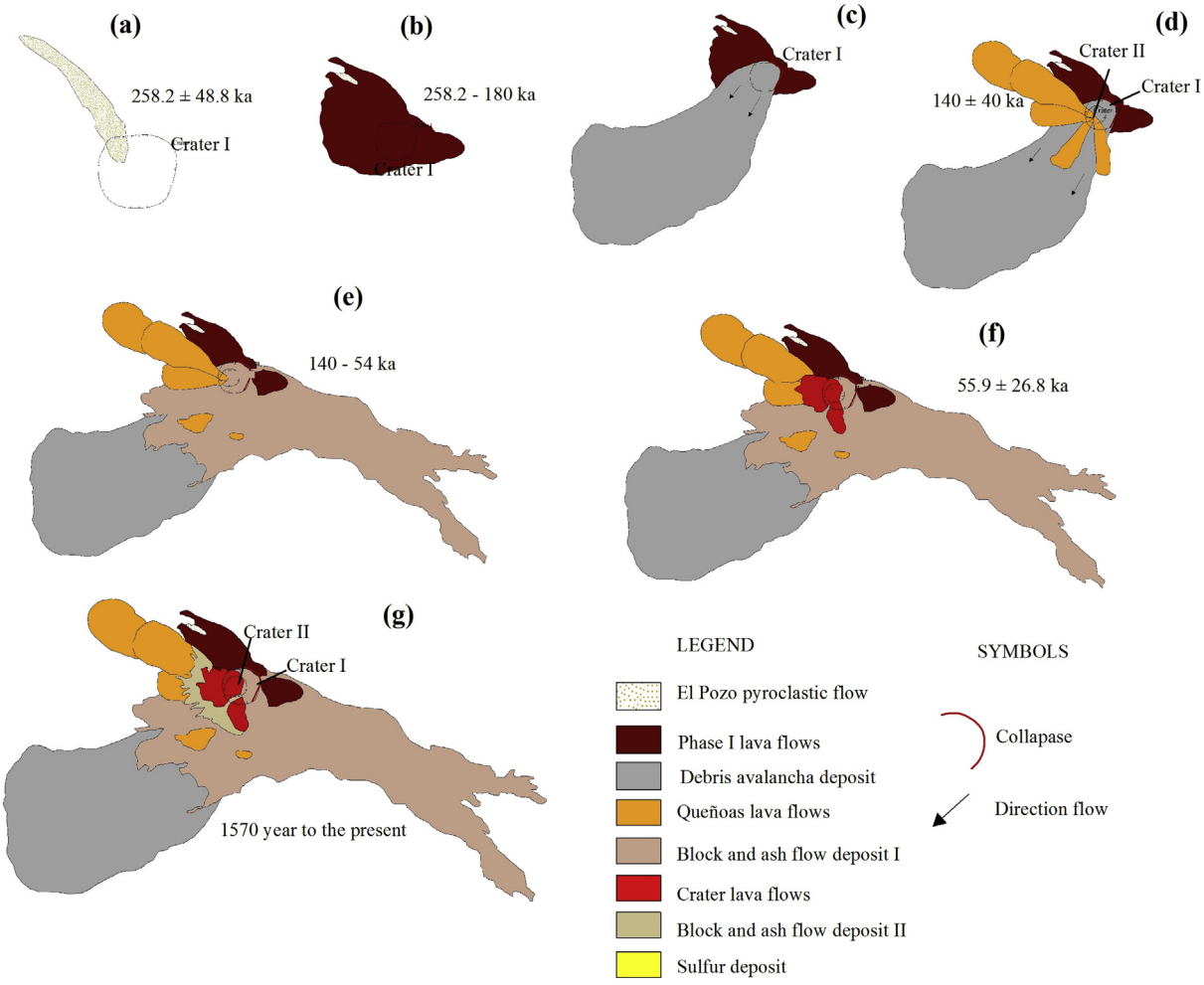

Fig. 12. Schematic temporal evolution of Irruputuncu, with units described in the main text. (a–c) Irruputuncu I. (d–g) Irruputuncu II.

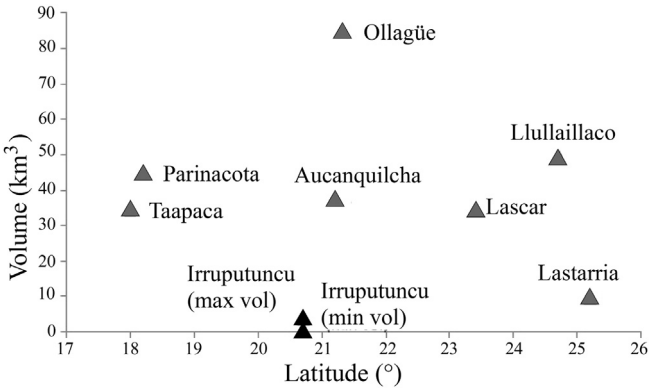

Fig. 13. Volume comparison between the Irruputuncu volcano and other volcanic systems in the Central Andes. Volume data from Feeley and Davidson (1994), Mathews et al. (1994), Richards and Villeneuve (2001), Clavero et al. (2004a and b), Klemetti and Grunder (2008), Naranjo (2010).

clinopyroxene. The Irruputuncu magmatic system shows small variations in magma composition, and in particular SiO_2 and K_2O concentrations increased slightly during Irruputuncu stage II.

Mingling features in juvenile clasts as well as disequilibrium textures in minerals give further insights into the magmatic processes, but a detailed discussion is beyond the scope of the paper. We note, however, that the banded pumice-scoria juvenile fragments in the El Pozo unit suggest that magma mixing occurred in the reservoir, as reported for instance for Lastarria volcano (Naranjo, 1992). The slight compositional variations of the mafic and silicic components could be produced by zonation prior to mixing or because mixing took place at more than one level on the magma reservoir (e.g. Lastarria volcano, Naranjo, 1992).

Most plagioclase phenocrysts, immersed in mostly vitrous groundmass, show resorbed edges and sieve textures, while hornblende and biotites phenocrysts show evidence of Fe oxidation, and pyroxene in their edges, which further suggests magma mixing (e.g. Lastarria volcano; Naranjo, 1992) at various stages of the Irruputuncu history. Rare occurrence of skeletic textures in some crystals (biotites) may indicate rapid cooling of the magma.

5.3. Volume estimation

The minimum volume of the Irruputuncu units is about 0.5 km^3, with a respective contribution of ~30% and ~70% for Irruputuncu I and Irruputuncu II, while the total volume of the edifice is ~4 km^3. Although our volume estimates are not accurate it is clear that Irruputuncu is very small compared to other recent volcanic systems in the same area as shown in Fig. 13 (e.g. 35 km^3 for Lascar, Gardeweg et al., 1998; 45 km^3 for Parinacota, Clavero et al., 2004; 37 km^3 for Aucanquilcha, Klemetti and Grunder, 2008).

6. Conclusion

The Irruputuncu volcano has been active for at least the last ~258 ± 49 ka and is one of the youngest volcanoes in the Central Andes. The volcanic system has a volume of about 4 km^3 and covers an area of ~23.8 km^2, making it one of the smallest active eruptive center of Central Andes. The first detailed geological map of Irruputuncu volcano that we provide in this study permits us to identify that the edifice was built during two main stages: Irruputuncu I and Irruputuncu II.

After an initial small explosive phase the eruptive activity was effusive and generated lava flows and lava domes from the old and now inactive crater I during Irruputuncu I. A major flank collapse evidenced by a widespread and well preserved debris avalanche deposit marked the end of Irruputuncu I, and Irruputuncu II began with emission of the voluminous Queñoas lava flows. Further activity was marked by successive events of dome growth and collapse as shown by block-and-ash flow deposits, and Crater II became the main active vent.

Magmas emitted by Irruputuncu volcano are of andesitic to trachy-andesitic composition and belong to the high-K calc-alkaline series typical of active volcanoes of the Central Andes. Major elements geochemistry indicates differentiation through fractional crystallization and co-crystallization of plagioclase and clinopyroxene. The main mineralogy assemblage corresponds to plagioclase, biotite, hornblende and pyroxenes. Minerals commonly present disequilibrium textures (sieve, reabsorption, skeletal) and replacement of minerals in the edges, which suggest events of magma mixing.

Acknowledgments

This research was financed by FONDECYT Project N°11100372, ECOS-CONICYT Project C11U01, Institut de Recherche pour le Développement (IRD), and the French Government Laboratory of Excellence initiative n°ANR-10-LABX-0006, the Région Auvergne and the European Regional Development Fund. This is Laboratory of Excellence ClerVolc contribution number 167. The authors are grateful to CEGA (Centro de Excelencia en Geotermia de los Andes), for the contribution to the dating. 40Ar/39Ar dates were obtained at Oregon State University (OSU) Argon Geochronology Lab, USA by Dr. Shan de Silva. Geochemical analyses were made at Laboratoire Magmas et Volcans in Clermont Ferrand, France, by Mhammed Benbakkar. Rock slides were done in the Departamento de Geología, Universidad de Atacama (Chile) by Jesús López. The authors gratefully acknowledge Tenencia Ujina for their hospitality and accommodation during the fieldtrip, Eduardo Valencia, Jerson Páez, Carla Bacigalupo, Francisco Gutierrez and Ornella Saltori for their friendship and invaluable help in the field. Pablo Samaniego provided useful comments on an earlier draft.

References

Aguilera, F., 2008. Origin and Evolution of Fluid in Volcanoes, Geothermal Fields and Thermal Discharges of Central Volcanic Zone in Northern Chile (17°43′S–25°10′S). Ph.D. thesis. Univ. Católica del Norte. Chile (in Spanish).
Allmendinger, R., Jordan, T., Suzanne, M., Isacks, B., 1997. The evolution of the altiplano-puna plateau of the Central Andes. Earth Planet 25, 139–174.
Baker, M.C.W., Francis, P.W., 1978. Upper Cenozoic volcanism in the Central Andes-ages and volumes. Earth Planet. Sci., Lett. 41, 175–187.
Bulletin of Global Volcanism Program, 1990. Volcanic Activivty Reports. Irruputuncu, vol. 15. BGVN. http://www.volcano.si.eduhttp://www.volcano.si.edu/, 03.
Bulletin of Global Volcanism Program, 1997. Volcanic Activivty Reports. Irruputuncu, vol. 22. BGVN. http://www.volcano.si.eduhttp://www.volcano.si.edu/, 07.
Calder, E.S., Cole, P.D., Dade, W.B., Druitt, T.H., Hoblitt, R.P., Huppert, H.E., Ritchie, L., Sparks, R.S.J., Young, S.R., 1999. Mobility of pyroclastic flows and surges at the Soufriere Hills Volcano, Montserrat. Geophys. Res. Lett. 26 (5), 537–540.
Clavero, E.J., Sparks, J.S.R., Pringle, S.M., Polanco, E., Gardeweg, C.M., 2004a. Evolution and volcanic hazards of Taapaca volcanic complex, Central Andes of northern Chile. J. Geol. Soc., Lond. 161, 603–618.
Clavero, E.J., Sparks, J.S.R., Polanco, E., Pringle, S.M., 2004b. Evolution of parinacota volcano, Central Andes, northern Chile. Rev. Geol. Chile 31, 317–347.
Clavero, J., Soler, V., Amigo, A., 2006. Caracterización preliminar de la actividad sísmica y de desgasificación pasiva de Volcanes activos de los Andes Centrales del Norte de Chile. XI congreso Geológico Chileno, pp. 7–11 (de Agosto).
Coira, B., Davidson, J., Mpodozis, C., Ramos, V., 1982. Tectonic and magmatic evolution of the Andes of Northern Argentina and Chile. Earth-Sci. Rev. 18, 303–332.
de Silva, S., Francis, P., 1991. Volcanoes of the Central Andes. Springer-Verlag, Berlin, p. 218, 219 figs.
de Silva, S., Davson, J., Croudace, I., Escobar, A., 1994. Volcanological and petrological evolution of volcan Tata Sabaya, SW Bolivia. J. Volcanol. Geotherm. Res. 55, 305–335.
Feeley, T., Davidson, J., 1994. Petrology of calc-alkaline lavas at Ollagüe and the origin of compositional dibersity at Central Andean stratovolcanes. J. Petrol. 35,

1295–1340.
Galli-Olivier, C., 1967. Pediplain in northern Chile and the Andean uplift. Science 158, 653–655.
Gardeweg, M., Sparks, S., Matthews, S., 1998. Evolution of Lascar volcano, northern Chile. London J. Geol. Soc. 155, 89–104.
González-Ferrán, O., 1995. Volcanes de Chile. Instituto Geográfico Militar, Santiago.
Grosjean, M., Geyh, M.A., Messerli, B., Schotterer, U., 1995. Late-glacial and early Holocene lake sediments, groundwater formation and climate in the Atacama Altiplano 22-24°S. J. Paleolimnol. 14, 241–252.
Hauser, A., 1997. Catastro y caracterización de las fuentes de aguas minerales y termales de Chile. N° 50. Servicio Nacional de Geología y Minería, p. 90.
Jordan, T.B., Grunder, L.A., 2004. Geochronology of age-progressive volcanism of the Oregon High Lava Plains: implications for the plume interpretation of Yellowstone. J. Geophys. Res. 109, B10202.
Klemetti, W.E., Grunder, L.A., 2008. Volcanic evolution of Volcán Aucanquilcha: a long-lived dacite volcano in the Central Andes of northern Chile. Bull. Volcanol. 70 (5), 633–650.
Mamani, M., Tassara, A., Wörner, G., 2008. Composition and structural control of crustal domains in the central Andes. Geochem. Geophys. Geosystems 9 (3), Q03006.
Mamani, M., Wörner, G., Sempere, T., 2010. Geochemical variations in igneous rocks of the Central Andean oricline (13°S to 18°S): tracing crustal thickening and magma generation through time and space. Geol. Soc. Am. Bull. 122 (1–2), 162–182.
Mathews, S.J., Jones, A.P., Gardeweg, M.C., 1994. Lascar volcano, northern Chile; evidence for steady-state disequilibrium. J. Petrol. 35, 401–432.
Matthews, S.J., Sparks, R.S.J., Gardeweg, M.C., 1999. The Piedras Grandes–Soncor eruptions, Lascar volcano, Chile; evolution of a zoned magma chamber in the Central Andean upper crust. J. Petrol. 40 (12), 1891–1919.
Naranjo, J.A., 1985. Sulphur flows at Lastarria volcano in the North Chilean Andes. Nature 313 (6005), 778–780.
Naranjo, J., 1992. Chemistry and petrological evolution of the Lastarria volcanic complex in north Chilean Andes. Geol. Mag. 129, 723–740.
Naranjo, J., 2010. Geología del complejo volcánico Lastarria, Región de Antofagasta. Carta geológica de Chile. Escala 1, 25.000. No 123.
Óladottir, B., Sigmarsson, O., Larsen, G., Devidal, J., 2011. Provenance of basaltic tephra from Vatnajökull subglacial volcanoes, Iceland, as determined by major- and trace-element analyses. Holocene 21, 1037–1048.
Richards, J.R., Villanueve, M., 2001. The Llullaillaco volcano, northwest Argentina: construction by Pleistocene volcanism and destruction by sector collapse. J. Volcanol. Geotherm. Res. 105, 77–105.
Rollison, H., 1993. Using Geochemical Data: Evaluation, Presentation, Interpretation. Longman Scientific & Technical Limited, Singapore.
Stern, C.R., Moreno, H., López-Escobar, L., Clavero, J.E., Lara, L.E., Naranjo, J.A., Skewes, M.A., 2007. Chilean volcanoes. Geol. Chile 149–180.
Tassi, F., Aguilera, F., Vaselli, O., Darrah, T., Medina, E., 2011. Gas discharges from four remote volcanoes in northern Chile (Putana, Olca, Irruputuncu and Alitar): a geochemical survey. Annals of Geophysics 54 (2).
Tassi, F., Aguilera, F., Vaselli, O., Medina, E., 2009. The magmatic-and hydrothermal-dominated fumarolic system at the active crater of Lascar volcano. Bull. Volcanol. 71, 171–183.
Vergara, H., Thomas, A., 1984. Hoja Collagua: región de Tarapacá, escala 1:250.000. N° 59. Servicio Nacional de Geología y Minería, p. 79.
Wörner, G., Harmon, R., Davidson, J., Moorbath, S., Turner, T., McMillan, N., Nye, C., Lopez-Escobar, L., Moreno, H., 1988. The Nevados de Payachata volcanic region 18°S/69°W, N. Chile. I. Geological, geochemical and isotopic observations. Bull. Volcanol. 30, 287–303.
Wörner, G., Moorbath, S., Harmon, R., 1992. Andean Cenozoic volcanic centers reflect basement isotopic domains. Geology 20 (12), 1103–1106.
Wörner, G., Hammerschmidt, K., Henjes-Kunst, F., Lezaun, J., Wilke, H., 2000. Geochronology (40Ar/39Ar, K-Ar and He-exposure ages) of Cenozoic magmatic rocks from northern Chile (18-22°S): implications for magmatism and tectonic evolution of the central Andes. n°2 Rev. Geol. Chile 27, 205–240.